



## OPEN ACCESS

## EDITED BY

Jamil S. Saad,  
University of Alabama at Birmingham,  
United States

## REVIEWED BY

Andrea Verna,  
Instituto de Innovación para la Producción  
Agropecuaria y el Desarrollo Sostenible  
(IPADS), Argentina  
Elizabeth Draganova,  
Emory University, United States

## \*CORRESPONDENCE

Gaetano Donofrio  
✉ gaetano.donofrio@unipr.it

RECEIVED 22 February 2023

ACCEPTED 12 April 2023

PUBLISHED 10 May 2023

## CITATION

Russo L, Capra E, Franceschi V, Cavazzini D,  
Sala R, Lazzari B, Cavarani S and Donofrio G  
(2023) Characterization of BoHV-4 ORF45.  
*Front. Microbiol.* 14:1171770.  
doi: 10.3389/fmicb.2023.1171770

## COPYRIGHT

© 2023 Russo, Capra, Franceschi, Cavazzini,  
Sala, Lazzari, Cavarani and Donofrio. This is an  
open-access article distributed under the terms  
of the [Creative Commons Attribution License  
\(CC BY\)](https://creativecommons.org/licenses/by/4.0/). The use, distribution or reproduction  
in other forums is permitted, provided the  
original author(s) and the copyright owner(s)  
are credited and that the original publication in  
this journal is cited, in accordance with  
accepted academic practice. No use,  
distribution or reproduction is permitted which  
does not comply with these terms.

# Characterization of BoHV-4 ORF45

Luca Russo<sup>1</sup>, Emanuele Capra<sup>2</sup>, Valentina Franceschi<sup>1</sup>,  
Davide Cavazzini<sup>3</sup>, Roberto Sala<sup>4</sup>, Barbara Lazzari<sup>2</sup>,  
Sandro Cavarani<sup>1</sup> and Gaetano Donofrio<sup>1\*</sup>

<sup>1</sup>Dipartimento di Scienze Medico Veterinarie, Università di Parma, Parma, Italy, <sup>2</sup>Istituto di Biologia e Biotecnologia Agraria, Consiglio Nazionale delle Ricerche IBBA CNR, Lodi, Italy, <sup>3</sup>Dipartimento di Scienze Chimiche, della Vita e della Sostenibilità Ambientale, Università di Parma, Parma, Italy, <sup>4</sup>Dipartimento di Medicina e Chirurgia, Università di Parma, Parma, Italy

Bovine herpesvirus 4 (BoHV-4) is a *Gammaherpesvirus* belonging to the *Rhadinivirus* genus. The bovine is BoHV-4's natural host, and the African buffalo is BoHV-4's natural reservoir. In any case, BoHV-4 infection is not associated with a specific disease. Genome structure and genes are well-conserved in *Gammaherpesvirus*, and the *orf45* gene and its product, ORF45, are one of those. BoHV-4 ORF45 has been suggested to be a tegument protein; however, its structure and function have not yet been experimentally characterized. The present study shows that BoHV-4 ORF45, despite its poor homology with other characterized *Rhadinivirus* ORF45s, is structurally related to Kaposi's sarcoma-associated herpesvirus (KSHV), is a phosphoprotein, and localizes in the host cell nuclei. Through the generation of an ORF45-null mutant BoHV-4 and its pararevertant, it was possible to demonstrate that ORF45 is essential for BoHV-4 lytic replication and is associated with the viral particles, as for the other characterized *Rhadinivirus* ORF45s. Finally, the impact of BoHV-4 ORF45 on cellular transcriptome was investigated, an aspect poorly explored or not at all for other *Gammaherpesvirus*. Many cellular transcriptional pathways were found to be altered, mainly those involving p90 ribosomal S6 kinase (RSK) and signal-regulated kinase (ERK) complex (RSK/ERK). It was concluded that BoHV-4 ORF45 has similar characteristics to those of KSHV ORF45, and its unique and incisive impact on the cell transcriptome paves the way for further investigations.

## KEYWORDS

herpesvirus, *Gammaherpesvirus*, ORF45, tegument protein, transcriptome

## 1. Introduction

Bovine herpesvirus 4 (BoHV-4) is a herpesvirus belonging to the *Gammaherpesvirinae* subfamily and *Rhadinivirus* genus. In some circumstances, BoHV-4 was isolated from cattle affected by different pathological entities, such as abortion, metritis, pneumonia, diarrhea, respiratory infection, and mammary pustular dermatitis. However, the pathogenic role of BoHV-4 remains unclear, and only a few investigators have successfully produced an experimental disease. Although BoHV-4's natural host is bovine, where it was found to be widespread in the population and persists in many individuals as an asymptomatic infection, BoHV-4 was isolated from other ruminant species too, and occasionally from lions, cats, and owl monkeys (Barahona et al., 1973; Bublot et al., 1991). Notably, BoHV-4 was found to be highly prevalent (higher than 68%) in African buffalo (*Syncerus caffer*). BoHV-4 isolated from buffalo diverged from BoHV-4 isolated from cattle ~730,000 years ago (Dewals et al., 2006), and thus African buffalo is considered to be the natural reservoir of the virus (Dewals et al., 2005). Experimentally, BoHV-4 was also shown to infect goats

(Moreno-Lopez et al., 1989), guinea pigs, and rabbits (Egyed et al., 1997). *In vitro*, BoHV-4 can replicate in primary cell cultures or cell lines from several host species, such as sheep, goats, swine, cats, dogs, rabbits, mink, horses, turkeys, ferrets, chickens, hamsters, rats, mice, monkeys, and human (Donofrio et al., 2002).

BoHV-4 has a B-type genome structure, according to the ICTV Virus Taxonomy classification of herpesviruses genome (Purdy et al., 2022), characterized by a long unique region (LUR) flanked by polyreplicative DNA (prDNA) elements, as for Kaposi's sarcoma-associated herpesvirus (KSHV), Saimirine gammaherpesvirus 2 (SaHV-2), Ateline gammaherpesvirus 3 (AtHV-3), Otarine gammaherpesvirus 4 (OtHV-4), and the other *Gammaherpesvirinae* (McGeoch et al., 2000; Li et al., 2005). So far, two strains of BoHV-4 have been fully sequenced and annotated, namely, the 66-p-347 American strain (Zimmermann et al., 2001) and the V. test European strain (Palmeira et al., 2011), showing a nucleotide identity of 99.55% on average. BoHV-4 genome coding capacity is represented by 79 *orf*s: 59 *orf*s coding for proteins containing conserved domain (CCD) and 20 *orf*s coding for proteins containing non-conserved domain (NCD; Zimmermann et al., 2001; Palmeira et al., 2011). Using complementary proteomic approaches, a BoHV-4 proteogenomic map, integrating genomic sequencing and proteomic analysis data, was generated by Lete et al. (2012). The results showed that all the 37 identified proteins mapped into previously annotated *orf*s. However, most of these genes and their products have not been structurally and functionally characterized for BoHV-4, including *orf45* gene and its product, ORF45 protein. ORF45 is conserved in the *Gammaherpesvirinae* subfamily; there is no *alpha*-, *beta*herpesvirinae, and cellular homolog for ORF45, and it was characterized only for KHSV (Atyeo and Papp, 2022), murine gammaherpesvirus-68 (MHV-68; Jia et al., 2005), and rhesus monkey rhadinovirus (RRV; Jia et al., 2005). In the present study, using the BoHV-4 genome cloned as a bacterial artificial chromosome (BAC; Donofrio et al., 2008), which allowed us to generate an *orf45* BoHV-4 null mutant and its pararevertant, BoHV-4 ORF45 was characterized and defined as an authentic ORF45, similarly to KSHV, MHV-68, and RRV ORF45.

## 2. Materials and methods

### 2.1. Bovine ORF45 structure prediction

The prediction of the complete BoHV-4 ORF45 protein tertiary structure by different *ab initio* prediction systems only led to low-score confidence structures. However, the N-terminal end of the bovine ORF45 was successfully predicted with the Swiss Model 3D structure prediction server (Waterhouse et al., 2018) by using the homologous portion of the ORF45 protein present in human herpesvirus 8 (PDB: 7opo) as a template. The predicted ORF45 bovine structure is 47 residues long (from amino acids 26 to 72) and displayed an RMSD value of 0.105 Å. The Modeler comparative modeling program (Webb and Sali, 2016) has been used to model the bovine ORF45 FxFP motif to the human corresponding one (PDB: 7opm) bound to ERK2. The ChimeraX software was used to display protein structures (Pettersen et al., 2021).

### 2.2. Cells

HEK (human embryonic kidney cells) 293 T (ATCC: CRL-11268), BEK (bovine embryo kidney; Istituto Zooprofilattico Sperimentale, Brescia, Italy; BS CL-94), BEK *cre*, expressing *cre* recombinase (Donofrio et al., 2008), and Madin–Darby bovine kidney (MDBK) cells (ATCC: CRL-6071) were maintained in complete Eagle's minimal essential medium (cEMEM: 1 mM sodium pyruvate, 2 mM of L-glutamine, 100 IU/ml of penicillin, 100 µg/ml of streptomycin, and 0.25 µg/ml of amphotericin B), supplemented with 10% FBS, and incubated at 37°C/5% CO<sub>2</sub> in a humidified incubator. All the supplements for the culture medium were purchased from Gibco.

### 2.3. Construct generation

pCMV-ORF45HA was generated by PCR amplifying BoHV-4 ORF45 from pBAC-BoHV-4-A DNA cut with EcoRI. The PCR amplification reaction was carried out in a final volume of 50 µl, containing 20 mM Tris-hydrochloride pH 8.8, 2 mM MgSO<sub>4</sub>, 10 mM KCl, 10 mM (NH<sub>4</sub>)<sub>2</sub>SO<sub>4</sub>, 0.1 mg/ml BSA, 0.1% (v/v) Triton X-100, 5% dimethyl sulfoxide (DMSO), 0.2 mM deoxynucleotide triphosphate, and 0.25 µM of each primer. A couple of primers, ORF45 NheI sense and ORF45HA SmaI antisense, were used (see Supplementary Table 1) to provide BoHV-4-ORF45 with a NheI site at its amino-terminal and a SmaI site and an HA tag at its carboxy-terminal. With 1U of Pfu recombinant DNA polymerase (Thermo Fisher Scientific), 100 ng of DNA was amplified over 35 cycles as follows: 1 min of denaturation at 94°C, 1 min of annealing at 60°C, and 50 s of elongation at 72°C. The amplicon ORF45HA was cut with NheI/SmaI and inserted into pEGFP-C1 (Clontech), which was cut with the same enzyme, to generate pCMV-ORF45HA.

pCMV-ORF45HA was then used as a template to amplify ORF45HA again with the same PCR parameters described above, with the following two primers: Fusion-XhoI sense and SmaI-HA antisense (Supplementary Table 1). This new amplicon was fused in frame with the GFP ORF, subcloning ORF45, cut with XhoI/SmaI in pEGFP-C1, and cut with the same enzymes, generating pEGFP-ORF45-HA.

pTZ-KanaGalK was generated by subcloning the 2,232-bp galactokinase prokaryotic expression cassette (GalK) and the kanamycin resistance expression cassette (Kana) into the pTZ57R shuttle vector (Thermoscientific), cut with KpnI/PstI (Franceschi et al., 2013). First, the targeting vector, pORF45Left-KanaGalK-RightORF45, was generated by the insertion of the ~700-bp left ORF45 homology region amplicon (ORF45A sense and antisense, see Supplementary Table 1), cut with EcoRI/KpnI, in pTZ-KanaGalK, which was cut with the same enzymes; in this intermediate construct, cut with PstI/HindIII, was subsequently sub-cloned the ~700 bp right ORF45 homology region amplicon (ORF45B sense and antisense; see Supplementary Table 1), cut with the same enzymes.

The retargeting vector, pORF45Left-CMVORF45HA-RightORF45 was obtained subcloning the CMVORF45HA-pA entire expression cassette, excised from AseI/MluI cut pCMV-ORF45HA, in pORF45Left-KanaGalK-RightORF45, deprived of KanaGalK selector cassette, through NdeI/MluI restriction digestion.

## 2.4. Transient transfection

HEK 293T cells were seeded into 25-cm<sup>2</sup> flasks ( $1 \times 10^6$  cells/flask) and incubated at 37°C with 5% CO<sub>2</sub>. When cells were sub-confluent, the culture medium was removed, and the cells were transfected with pCMV-ORF45HA or pEGFP-C1 (a mock control) using polyethylenimine (PEI) transfection reagent (Polysciences, Inc.). Briefly, 7.5 µg of DNA were mixed with 18.75 µg of PEI (1 mg/ml; ratio 1:2.5 DNA:PEI) in 500 µl of Dulbecco's modified essential medium (DMEM) with high glucose (Euroclone) without serum. After 15 min of incubation at room temperature, 2,000 µl of medium without serum was added, and the transfection solution was transferred to the cells (monolayer) and left for 6 h at 37°C with 5% CO<sub>2</sub>, in a humidified incubator. The transfection mixture was then replaced with fresh cEMEM medium with 10% FBS and incubated for 24 h at 37°C with 5% CO<sub>2</sub>. To analyze the subcellular localization of BoHV-4 ORF45, HEK 293T cells were also transfected with pEGFP-ORF45-HA or pEGFP-C1 as a mock control. The cells were counterstained with 4',6-diamidino-2-phenylindole (DAPI; Thermo Scientific) and observed with a confocal microscope (Leica Microsystems) 24 h after the transfection.

## 2.5. Immunoblotting

Western immunoblotting analysis was performed on protein cell extracts from 25-cm<sup>2</sup> flasks of HEK 293T cells transfected with pCMV-ORF45HA or mock transfected. For protein extraction, 100 µl of cell extraction buffer (50 mM Tris-HCl, 150 mM NaCl, and 1% NP-40; pH 8) was added to each pellet, and total protein quantification was performed using the BCA Protein Assay Kit (Pierce™, Thermo Fisher Scientific). Before immunoblotting analysis, pCMV-ORF45HA-transfected cell extract was enriched in phosphorylated protein, passing through a phosphoprotein chelating metal resin enrichment kit (Pierce, Thermo Scientific), following the protocol suggested by the manufacturers. Different amounts of protein samples were electrophoresed on 10% SDS-PAGE and then transferred to PVDF membranes (Millipore, Merck) by electroblotting. The membrane was blocked in 5% skimmed milk (BD), incubated for 1 h with primary mouse monoclonal antibody anti-HA tag (G036; Abm Inc.), diluted 1:10,000, and then probed with horseradish peroxidase-labeled anti-mouse immunoglobulin (A9044; Sigma), diluted 1:15,000, and finally visualized by enhanced chemiluminescence (Clarity Max Western ECL substrate, Bio-Rad).

## 2.6. BAC recombineering and selection

Recombineering was performed as previously described (Warming et al., 2005) with some modifications. For heat-inducible homologous recombination in SW102 *Escherichia coli* (*E. coli*), containing the BoHV-4-A genome, cloned as a BAC, pBAC-BoHV-4-A, was used the double selector targeting cassette Left-KanaGalK-Right, which was excised from the plasmid backbone pORF45Left-KanaGalK-RightORF45, cut with EcoRI/HindIII. After recombineering, only those colonies that were kanamycin- and chloramphenicol positive were kept and grown overnight in 5 ml of LB containing 12.5 µg/ml of chloramphenicol or 50 µg/ml of kanamycin. BAC-DNA was purified and analyzed through HindIII restriction enzyme digestion. DNA was then separated by electrophoresis in a 1% agarose gel, stained with ethidium bromide, and visualized through UV light. SW102 bacteria containing the BAC-BoHV-4-A-ΔORF45KanaGalK genome were also grown, heat-induced, and electroporated with HindIII-linearized pORF45Left-CMVORF45HA-RightORF45 in the retargeting step. For the counter-selection step, only the colonies that grew on chloramphenicol and not on kanamycin were kept and grown overnight in 5 ml of LB containing 12.5 µg/ml of chloramphenicol. BAC-BoHV-4-A-revORF45HA DNA was purified and analyzed through HindIII restriction enzyme digestion for CMVORF45HA locus fragment targeted integration. Original, more detailed protocols for recombineering can also be found on the recombineering website (<https://redrecombineering.ncifcrf.gov/>).

## 2.7. Cell culture electroporation and recombinant virus reconstitution

BEK or BEK *cre* cells were maintained as a monolayer with cEMEM growth medium with 10% FBS. When cells were sub-confluent (70–90%), they were split into a fresh culture flask (i.e., every 3–5 days) and were incubated at 37°C in a humidified atmosphere of 95% air and 5% CO<sub>2</sub>. pBAC-BoHV-4-A, pBAC-BoHV-4-A-revORF45HA, and pBAC-BoHV-4-A-ΔORF45KanaGalK DNAs (5 µg) were electroporated in 600 µl DMEM high without serum (Biorad, Gene Pulser XCell, 270 V, 960 mF, 4-mm gap cuvettes) into BEK and BEK *cre* cells from a confluent 25-cm<sup>2</sup> flask. Electroporated cells were transferred to new flasks, the medium was replaced with fresh cEMEM after 24 h, and cells were split in the ratio 1:2 when they reached confluence at 2 days post-electroporation. Cells were grown until the appearance of the cytopathic effect (CPE).

## 2.8. Viruses and viral replication

BoHV-4-A and BAC-BoHV-4-A-revORF45 were propagated by infecting confluent monolayers of BEK or MDBK cells at a multiplicity of infection (MOI) of 0.5 tissue culture infectious doses 50 (TCID<sub>50</sub>) per cell and maintained in cEMEM with only 2% FBS for 2 h. The medium was then removed and replaced with

fresh cEMEM with 10% FBS. When CPE affected the majority of the cell monolayer (~72 h post infection), the virus was prepared by freezing and thawing cells three times and pelleting the virions through a 30% sucrose cushion, as previously described (Donofrio et al., 2006). Virus pellets were then resuspended in cold cEMEM without FBS. Viral pellets that were loaded in SDS-PAGE gel were resuspended in 100  $\mu$ l of cell extraction buffer (50 mM Tris-HCl, 150 mM NaCl, and 1% NP-40; pH 8) and heat-denatured. TCID<sub>50</sub> was determined on BEK cells by limiting dilution.

## 2.9. Viral growth curves

BEK cells were infected with BoHV-4-A and BAC-BoHV-4-A-revORF45 at an MOI of 0.1 TCID<sub>50</sub>/cell and incubated at 37°C for 3 h. Infected cells were washed with serum-free EMEM and then overlaid with cEMEM with 10% FBS. The supernatants of infected cultures were harvested at scheduled time points (24, 48, 72, and 96 h post infection), and the amount of infectious virus was determined by limiting dilution on BEK or MDBK cells. The viral titer differences between each time point are the averages of triplicate measurements  $\pm$  standard errors of the mean ( $p > 0.05$  for all time points as measured by Student's *t*-test).

## 2.10. RNA isolation

Until extraction, five million cells were resuspended in 1 ml of Trizol and stored at  $-80^{\circ}\text{C}$ . Total RNA was isolated by the NucleoSpin miRNA kit (Macherey-Nagel), using the protocol combined with TRIzol lysis (Invitrogen) and small and large RNA recovery in one fraction. The concentration and quality of RNA were determined by Agilent 2100. The isolated RNAs were stored at  $-80^{\circ}\text{C}$  until use.

## 2.11. Library preparation and sequencing

RNA samples (RIN  $> 7.5$ ) from four replicates ( $n = 4$ ) for each condition (control and treated) were used for library preparation. RNA-Seq libraries were obtained using the Illumina TruSeq RNA Sample Preparation Version 2 kit. Concentration and quality checks of libraries were determined using Agilent 2100 bioanalyzer. Sequencing was performed on a single lane of Illumina HiSeq X, 150 cycles paired end.

## 2.12. Data analysis

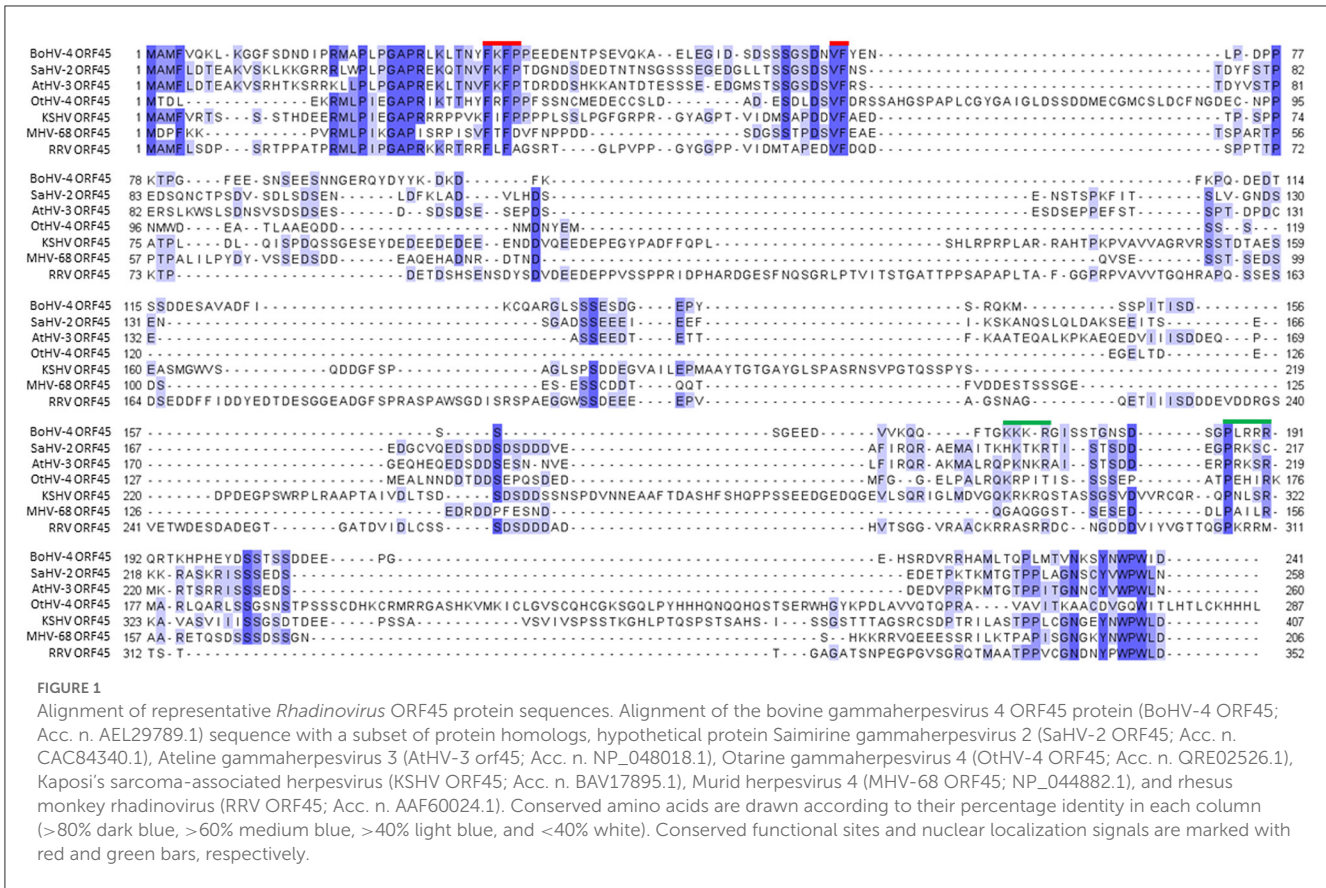
RNA-Seq analysis was run with the nf-core/rnaseq version 3.8.1 pipeline (<https://nf-co.re/rnaseq>). The pipeline integrates TrimGalore version 0.6.7 for sequence trimming and STAR version 2.7.10a (Dobin et al., 2013) for sequence alignment.

Sequences were aligned to the human GRCh38.p13 reference genome. Salmon version 1.5.2 (<https://combine-lab.github.io/salmon/>) was used to quantify alignments to gene regions. The EdgeR Bioconductor package version 3.6 (Bioconductor, <https://bioconductor.org/packages/release/bioc/html/edgeR.html>) was used to estimate differential expression between control and treated samples. Hierarchical cluster analysis was performed with Genesis (Sturn et al., 2002).

## 3. Results

### 3.1. BoHV-4 ORF45 has a relatively low protein homology with other *Rhadinovirus* ORF45s and is structurally related to KHSV ORF45

BoHV-4 ORF45 gene, in the genome of BoHV-4, has the same locus position (*orf44-orf45-orf46-orf47*) as the ORF45 gene belonging to the viruses of the same genus, *Rhadinovirus*. However, ORF45 nucleotide sequences and their protein products often have a weak percentage of identity between them. In fact, at the protein level, the BoHV-4 ORF45 identity percentage was identified to be 24.9, 21.74, and 23.38 with KSHV, RRV, and MHV68, respectively (Figure 1). ORF45 genes have been sequenced and annotated, and their protein products have been deduced in all *Rhadinovirus* isolates to date; however, only KSHV ORF45 has been characterized in terms of structure (Alexa et al., 2022). BoHV-4 ORF45 protein sequence BLAST analysis identified partial low-score homology sequences but no hits in the pdb database. In contrast, HHpred analysis found in the KHSV ORF45 N-terminal fragment, which contains the binding domain for p90 ribosomal S6 kinase (RSK) and signal-regulated kinase (ERK) complex (Alexa et al., 2022), a significant homology (~30%) with BoHV-4 ORF45, which was used as a potential structural template (Figure 2A). Thus, the N-terminal structure of BoHV-4 ORF45 was successfully predicted with the Swiss Model 3D prediction server (Waterhouse et al., 2018). KHSV ORF45 takes over the host mitogen-activated protein kinase (MAPK) pathway-signaling cascade to promote the viral life cycle by forming a ternary complex with extracellular signal-regulated ERK and RSK kinase heterodimers, which are important components of the downstream epidermal growth factor (EGF)/Ras/ERK pathway. The binding of two distinct N-terminal KHSV ORF45 linear binding motifs to ERK and RSK causes their permanent activation by preventing the dephosphorylation of the two kinases. As shown in Figure 2B, the predicted BoHV-4 ORF45 structure is well-superimposed (RMSD 0.1 Å) on the corresponding KHSV ORF45 ortholog bound to RSK2 kinase (Figure 2B). Furthermore, the key Val and Phe (VP) interacting motif residues are also conserved in the BoHV-4 ORF45 and well fit the hydrophobic pocket located in the N-terminal of AGC-type kinase domain (NTK) of RSK (Figure 2C). Therefore, BoHV-4 ORF45 protein is expected to bind to phosphorylated ERK2, since the substrate-mimicking FxFP motif present in the KHSV ORF45 is also conserved in the BoHV-4 ORF45 and well fits the hydrophobic F-site of ERK2 (Figure 2D). Both ERK2 and RSK2 are highly conserved among mammals, and the corresponding bovine protein sequences are 99.7% identical



to the corresponding human ortholog. Based on this evidence, it is therefore expected that the two conserved VP and FxPP N-terminal linear motifs of BoHV-4 ORF45 could bind to bovine RSK2 and ERK2 kinases and maintain them in a sustained activated state, thus hijacking the MAPK host pathway and favoring the viral infection.

### 3.2. BoHV-4 ORF45 is a phosphoprotein

BoHV-4 ORF45 has an *in silico* predicted length, starting from its nucleotide sequence (*orf45*; Zimmermann et al., 2001; Palmeira et al., 2011), of 241 aminoacidic residues, an isoelectric point (IP) of 4.76, a mass of 27.142 kDa, an aliphatic index of 40.46, and is lacking a putative signal peptide. Hence, in general, BoHV-4 ORF45 could be described as an intracellular soluble acidic protein. Since BoHV-4 ORF45 has not been characterized so far, and consequently no specific antibodies have been developed, to follow its expression in mammalian cells, a carboxy-terminal HA-tagged ORF45, pCMV-ORF45HA, was constructed. Surprisingly, BoHV-4 ORF45 had an SDS-PAGE migration almost double than predicted, ~55 kDa (Figure 3A). This is probably due to some post-transcriptional modifications and agrees with what was found for MHV68 ORF45 (Jia et al., 2005) and KSHV ORF45 (Zhu and Yuan, 2003). Glycosylation sites were not predicted and not identified when BoHV-4 ORF45 was treated with endoglycosidases (data not shown). However, BoHV-4 ORF45 analysis using NetPhos-3.1

(Blom et al., 1999, 2004) indicated the presence of several phosphorylation sites, where serine and threonine were mainly involved, but tyrosine also appeared with a lower frequency and score (Figure 3B). Finally, by transient transfection and in the absence of infection, BoHV-4 ORF45 phosphorylation, in pCMV-ORF45HA transfected cell extracts, was confirmed by a phosphoprotein affinity resin that retained BoHV-4 ORF45 (Figure 3C).

### 3.3. BoHV-4 ORF45 localizes to the cell nucleus

As predicted by PSORT sequence analysis (Nakai, 2000), a nuclear localization signal was identified in BoHV-4 ORF45 (78%;  $K = 9/23$ ; consensus: KKRR at 172 and PLRRRQR at 187) but not a nuclear export signal as detected in KSHV ORF45 (Li and Zhu, 2009). For examining the capability of BoHV-4 ORF45 to localize to the nucleus independently from other viral protein backgrounds, GFP *orf* was fused in frame with BoHV-4 HA-tagged ORF45 *orf*, and a plasmid construct, pEGFP-ORF45-HA, was generated. pEGFP-ORF45-HA transfected cells were visualized with a confocal microscope 24 h post transfection; as predicted, a GFP fluorescent signal was well-observed within the cell nuclei (Figures 4A–D). Therefore, BoHV-4 ORF45 delivered GFP, known to be a cytoplasmic protein (Figure 4D), into the cell nucleus.

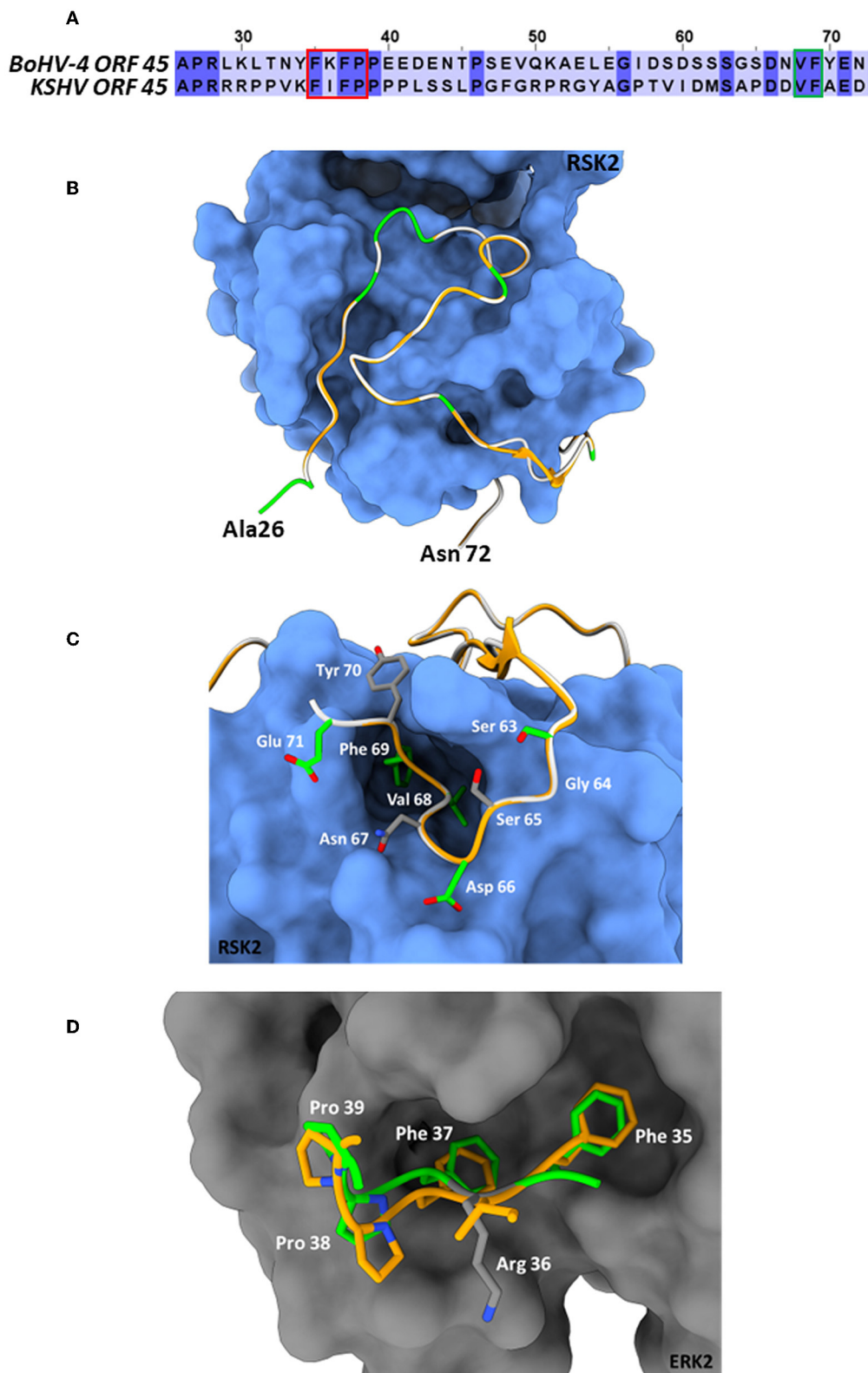
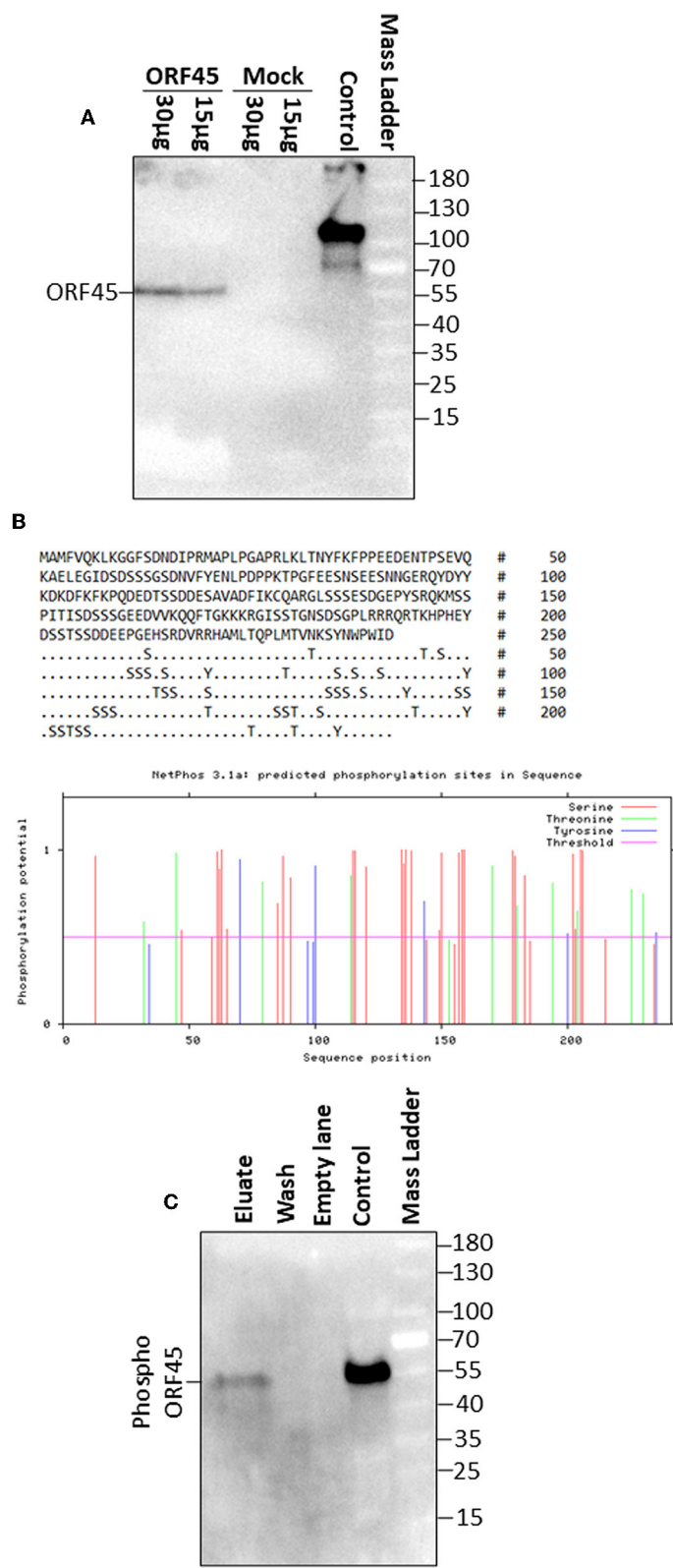
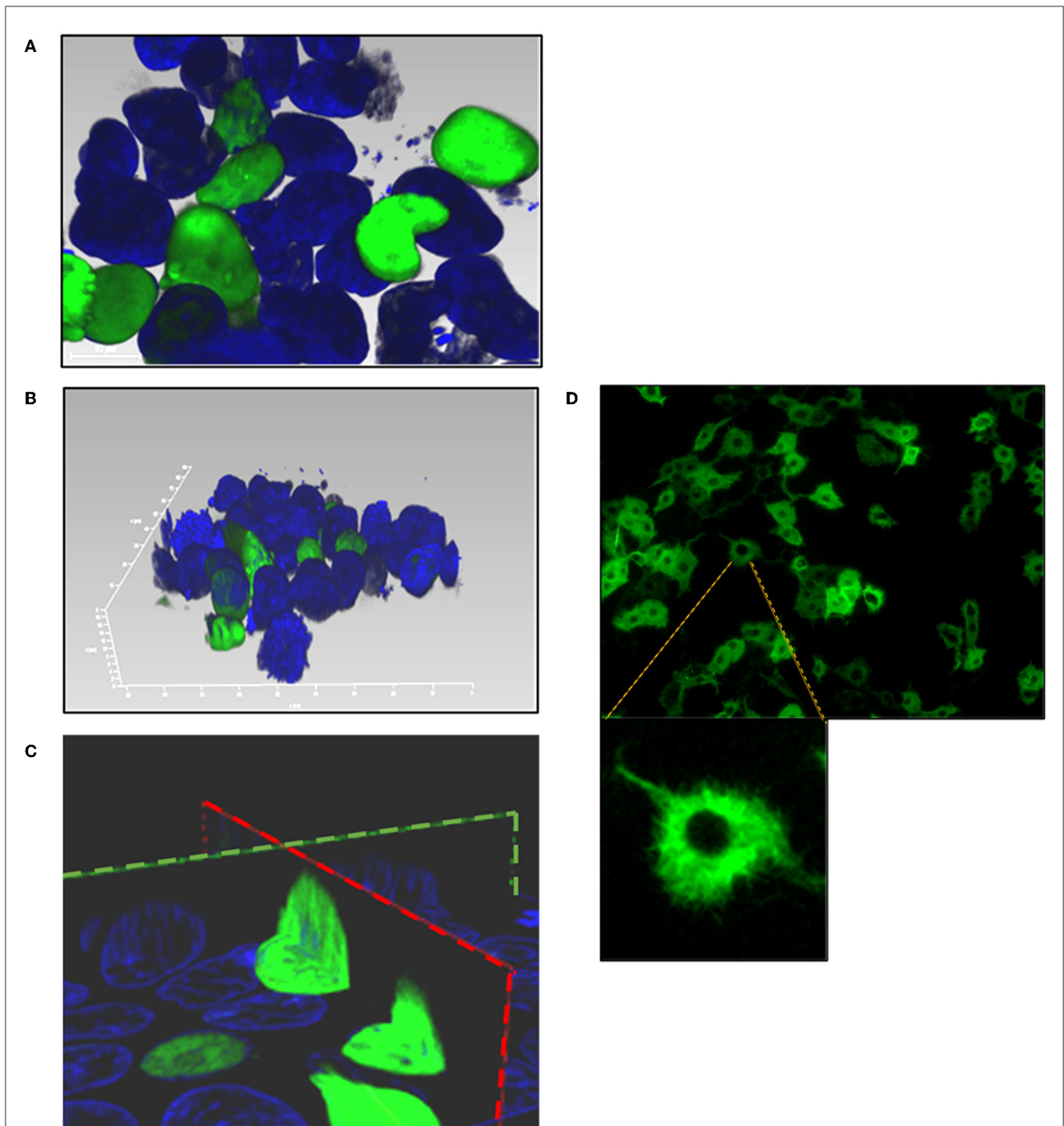


FIGURE 2

BoHV-4 ORF45 predicted structure. **(A)** Amino acid sequence alignment between the BoHV-4 ORF45 (upper sequence, from aa. 26 to 72) and the corresponding residues of KSHV ORF45 ortholog (lower sequence). The conserved amino acids are shown on a dark-blue background. The red and green rectangles indicate the ORF45 VP-interacting motif and the substrate-mimicking FxFP motif, respectively. **(B)** The predicted Ca backbone of BoHV-4 ORF45 (in green, the conserved residues; in white, the non-conserved residues) is superimposed onto the human ORF45 Ca structure (in orange) bound to RSK2 (protein surface in blue; PDB: 7opm). The N- and C- termini of the bovine protein are labeled. **(C)** Particularly of the predicted BoHV-4 ORF45 3D structure (Ca and side chains) superimposed onto Ca KSHV ORF45 Val-Phe binding motif bound to RSK2. Color code of Ca chains as in **(B)**, while the bovine ORF45 side chains are rendered in green/CPK or gray/CPK sticks, if conserved or non-conserved, respectively. **(D)** Superposition of the predicted BoHV-4 ORF45 3D structure FxFP motif onto the corresponding human ORF45 (PDB: 7opm) residues bound to the hydrophobic F-site of ERK2 (protein surface in gray; PDB: 7opm). Human ORF45 Ca and side chains are in orange/CPK sticks; bovine Ca and side chain residues are in green/CPK or gray/CPK sticks if conserved or not, respectively.



**FIGURE 3** BoHV-4 ORF 45 phosphorylation. **(A)** Western immunoblotting of pCMV-ORF45HA (ORF45) and pEGFP-C1 (Mock) transfected cell protein extracts (30 and 15 µg of total protein extract). A positive antibody control was established with an HA-tagged unrelated protein. **(B)** BoHV-4 ORF45 protein sequence along with serine (S), threonine (T), and tyrosine (Y) residues potentially phosphorylated as predicted by NetPhos 3.1, where the scores above 0.500 indicate positive predictions. **(C)** Western immunoblotting of concentrated eluate and wash of pCMV-ORF45HA transfected cell extract, passed through a phosphoprotein chelating metal resin. A positive antibody control was established with pCMV-ORF45HA transfected cell extract that was not passed through the resin.



**FIGURE 4**

Subcellular localization of BoHV-4 ORF45. Cells were transfected with a construct, pEGFP-ORF45-HA, where GFP *orf* was fused to the 5' end of BoHV-4ORF45 *orf*. Transfected cells were counterstained with DAPI and observed with a confocal microscope 24 h post transfection. **(A)** 2D image of pEGFP-ORF45-HA transfected cells where GFP-ORF45 is localized within the nuclei (green). **(B)** 3D image of cell nuclei containing GFP-ORF45 (green). **(C)** Sagittal (green dashed line) and transverse (red dashed line) images of cell nuclei containing GFP-ORF45. **(D)** 2D image of pEGFP-C1 transfected cell control, where GFP is predominantly localized within the cytoplasm (green).

### 3.4. BoHV-4 ORF45 is an essential gene for BoHV-4 lytic replication and is associated with the virus

To investigate the role of the BoHV-4 ORF45 gene during viral lytic replication, the BoHV-4 ORF45 gene was deleted by

site-specific insertional mutagenesis mediated by heat-inducible homologous recombination (Warming et al., 2005) in the genome of a BoHV-4 cloned as a BAC (BAC-BoHV-4-A). BAC-BoHV-4-A was originally derived from a non-pathogenic strain of BoHV-4 isolated from the milk cellular fraction of a healthy cow (Donofrio et al., 2008). The targeting cassette, Left-KanaGalK-Right, which

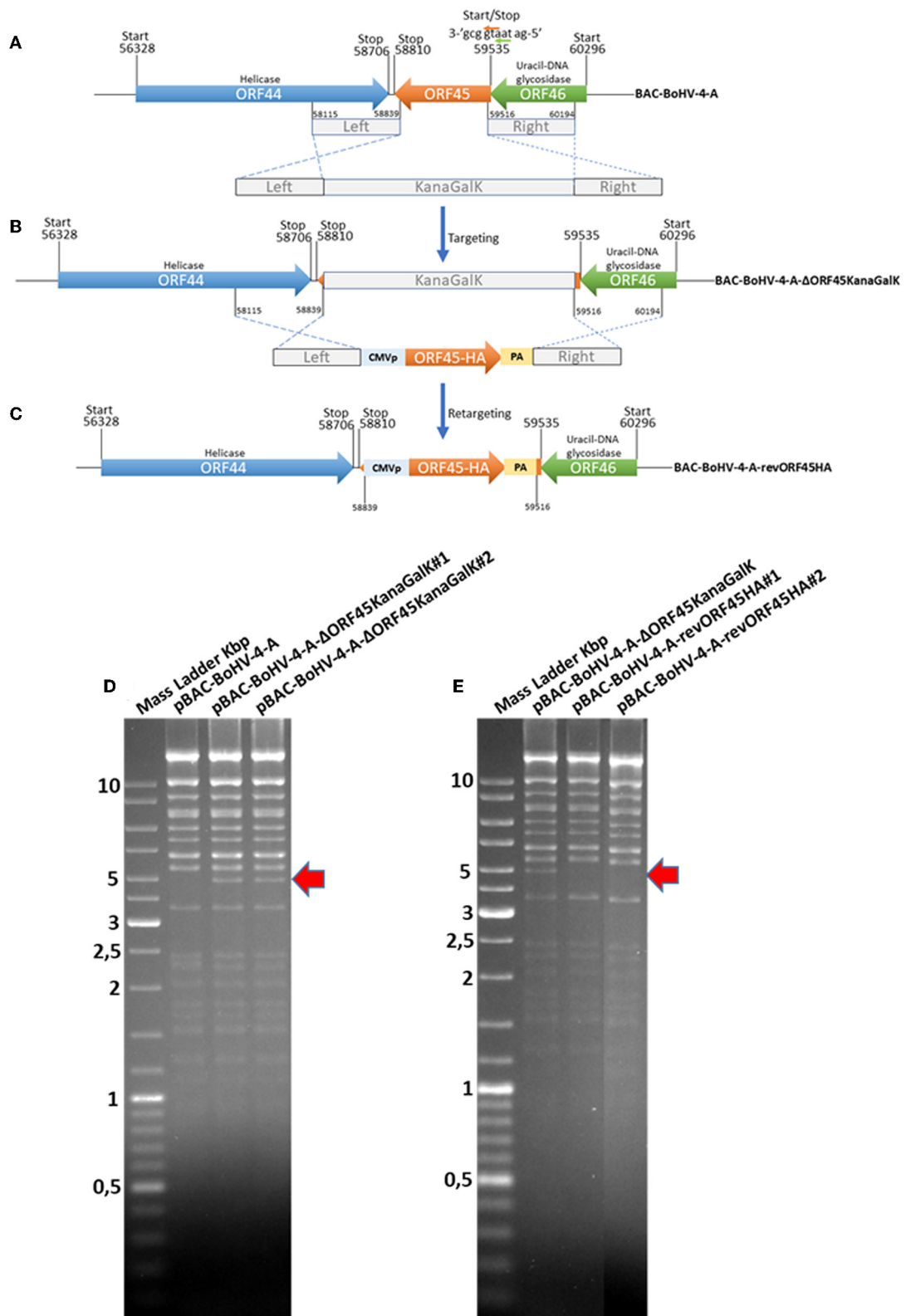


**FIGURE 5**  
 Overall strategy to disrupt the BoHV-4 ORF45 gene via heat-inducible homologous recombination. **(A, B)** Diagram (not to scale) of the BoHV-4 ORF45 gene (orange arrow; nucleotide 59535 and 58810) positioned between ORF 44 (blue arrow; nucleotide 56328 and 58706) and ORF46 (green arrow; nucleotide 60296 and 59535). The last nucleotide of the ORF46 stop codon and the first nucleotide of the ORF45 start codon (a) are overlapped. ORF46 and ORF45 are transcribed in the opposite direction to ORF44 [based on the complete genome published sequence (GenBank accession number AF318573)]. The 2,232-bp Kana/GalK selectable DNA stuffer (gray), flanked by left (nucleotide 58115 and 58839; 724 bp) and right homologous regions (nucleotide 58516 and 60194; 678 bp), was introduced between the positions 58839 and 59516, deleting most of the ORF45 sequence but leaving intact ORF44 and ORF46, and BoHV-4-A-ΔORF45KanaGalK was generated. **(B)** CMVORF45HA expression cassette flanked by (Continued)

## FIGURE 5 (Continued)

the left and right homologous regions (gray) was used to replace 2,232-bp Kana/GalK selectable DNA stuffer (gray), and BoHV-4-A-revORF45HA was so generated (C). (D) HindIII restriction enzyme profile of two representative pBAC-BoHV-4-A- $\Delta$ ORF45KanaGalK clones (1 and 2) compared with the parental pBAC-BoHV-4-A. The diagnostic band, indicated by a red arrow, was well-observable in pBAC-BoHV-4-A- $\Delta$ ORF45KanaGalK with respect to pBAC-BoHV-4-A. (E) HindIII restriction enzyme profile of two representative pBAC-BoHV-4-A-revORF45HA clones (1 and 2) compared with the derivative pBAC-BoHV-4-A- $\Delta$ ORF45KanaGalK. The missing band, indicated by a red arrow, was well-observable in pBAC-BoHV-4-A-revORF45HA with respect to pBAC-BoHV-4-A- $\Delta$ ORF45KanaGalK.

contains the 2,232-bp KanaGalK DNA stuffer double selecting cassette (Donofrio et al., 2007) flanked by two BoHV-4 ORF45 gene homologous flanking regions, was generated to mediate insertion and deletion of the BoHV-4 ORF45 coding region. The BoHV-4 ORF45 gene is transcribed from the opposite BoHV-4 genome DNA strand (Zimmermann et al., 2001; Palmeira et al., 2011) like ORF46 but in contrast to ORF44 (Figure 5A). Therefore, although a large deletion and insertion were made, this should not affect ORF44 and ORF46 transcription/translation, and the viral phenotype obtained should be exclusively due to the loss of ORF45. The Left-KanaGalK-Right targeting cassette was excised from the plasmid backbone and electroporated into SW102 *E. coli* containing pBAC-BoHV-4-A, to generate pBAC-BoHV-4-A- $\Delta$ ORF45KanaGalK (Figure 5B). Selected targeted clones were analyzed by PCR, sequencing (data not shown), and HindIII restriction enzyme digestion (Figure 5D). Furthermore, to stress that the authenticity of pBAC-BoHV-4-A- $\Delta$ ORF45KanaGalK phenotype was exclusively caused by the loss of ORF45 and not a mere artifact, a control BoHV-4 with a carboxy-terminal HA-tagged ORF 45 that was transcriptionally driven in the opposite direction to the natural ORF45 by a heterologous promoter (CMV) was generated. The retargeting cassette, Left-CMV-ORF45HA-Right, was excised out from the plasmid backbone and electroporated into SW102 *E. coli* containing pBAC-BoHV-4-A- $\Delta$ ORF45KanaGalK and pBAC-BoHV-4-A-revORF45HA (Figure 5C). Again, selected targeted clones were analyzed by PCR, sequencing (data not shown), and HindIII restriction enzyme digestion (Figure 5E). When pBAC-BoHV-4-A- $\Delta$ ORF45KanaGalK and pBAC-BoHV-4-A-revORF45HA were electroporated into BEK or BEK/cre cells to excise out the BAC cassette, plaques from the viable virus were obtained only on pBAC-BoHV-4-A-revORF45HA transfected cell monolayers but not on those transfected with pBAC-BoHV-4-A- $\Delta$ ORF45KanaGalK (Figure 6A). ORF45 deletion rendered BoHV-4-A unable to be reconstituted and productively replicated; such a phenotype was rescued by CMV-ORF45HA expression cassette (Figure 6B), thus showing ORF45's indispensability in the context of BoHV-4 lytic replication and in line with data obtained for KHSV ORF45 (Fu et al., 2015) and MHV68 ORF45 (Jia et al., 2005). Since BoHV-4-A-revORF45HA infectious virus produced an HA-tagged form of ORF45, detectable by an anti-HA mAb (Figure 6C), it was of interest to know if BoHV-4 ORF45 is associated with the virus as previously observed by Lete et al. (2012) in a proteomic analysis setting. As expected, when CsCl<sub>2</sub> gradient-purified virus was analyzed by SDS-PAGE and Western blotting with an anti-HA mAb, a specific band corresponding to ORF 45 was evident (Figure 6D).

### 3.5. BoHV-4 ORF45 expression alters the cellular transcriptome

Since BoHV-4 ORF45 possesses an acidic domain (between amino acids 40 and 66), is phosphorylated, and localizes into the cell nucleus, BoHV-4 ORF45 could also take part, perhaps indirectly through protein/protein interactions with other transcription factors, in a transcriptional regulatory network. To test this hypothesis, a comparative transcriptome analysis, by transient transfection and in the absence of infection, of cells expressing BoHV-4 ORF45 vs. BoHV-4 ORF45-unexpressing cells, was performed.

RNA-Seq analysis generated an average of 55.8 M (111.56 M paired reads) reads per sample, with ~81.4% of the total reads that were correctly mapped on the human reference genome (Supplementary Table 2, for statistics). A total of 30,738 unique genes were present in both groups, although 94 and 190 genes were only detected in treated and control samples, respectively (Figure 7A). The principal component analysis (PCA) separates control vs. treated samples (Figure 7B). A total of 984 differentially expressed genes (DEGs; FDR < 0.05) were identified (Figure 7C and Supplementary Table 3). Biological pathway analysis was performed for highly significant DEGs ( $n = 113$ , FDR < 0.01, and LogFC < |0.5|). Gene Ontology (GO) analysis showed variation in genes involved in the mitotic DNA damage checkpoint, the response to DNA damage by p53, and the pathway restricted to SMAD phosphorylation (Figure 8A and Supplementary Table 4). Reactome pathway database interrogation identified genes related to TP53 regulation of the cell cycle, kinase-mediated activation of nuclear transcription, and DNA damage senescence response (Figure 8B and Supplementary Table 4). This is in complete agreement with KSHV ORF45 functions (Atyeo and Papp, 2022) and interaction with p90 ribosomal S6 kinase (RSK) and signal-regulated kinase (ERK) complex.

## 4. Discussion

A herpesviral virion is generally composed of three electron microscopy morphologically distinct structures: an envelope, a capsid, and an electron-dense material defined as the tegument, located between the envelope and the capsid (Roizmann et al., 1992). Proteomic analysis of BoHV-4 mature virions, identified five envelope proteins, nine capsid proteins, and 13 tegument proteins (Lete et al., 2012). Among the tegument proteins, ORF45 was one of the most abundant. The criteria utilized to characterize BoHV-4

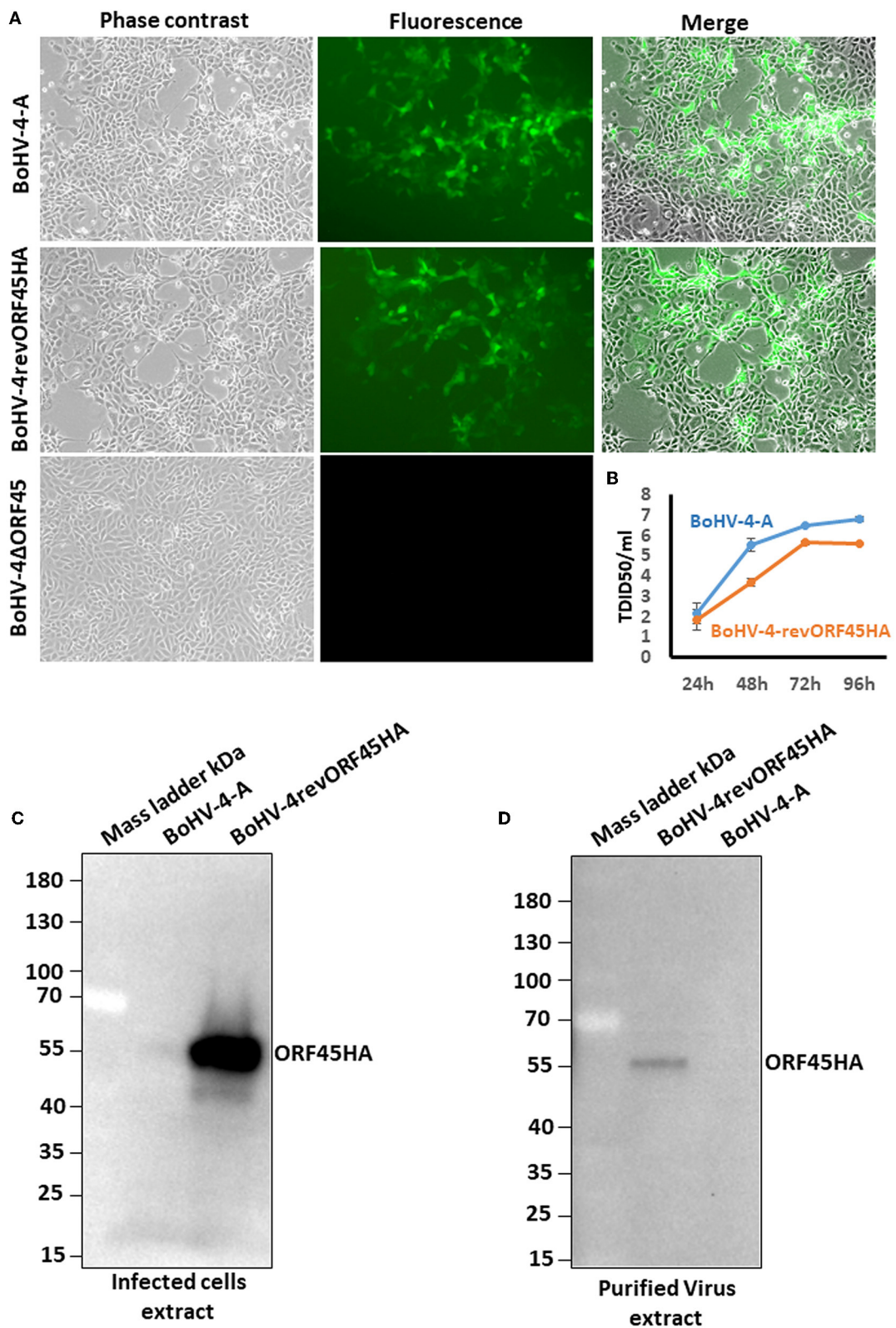
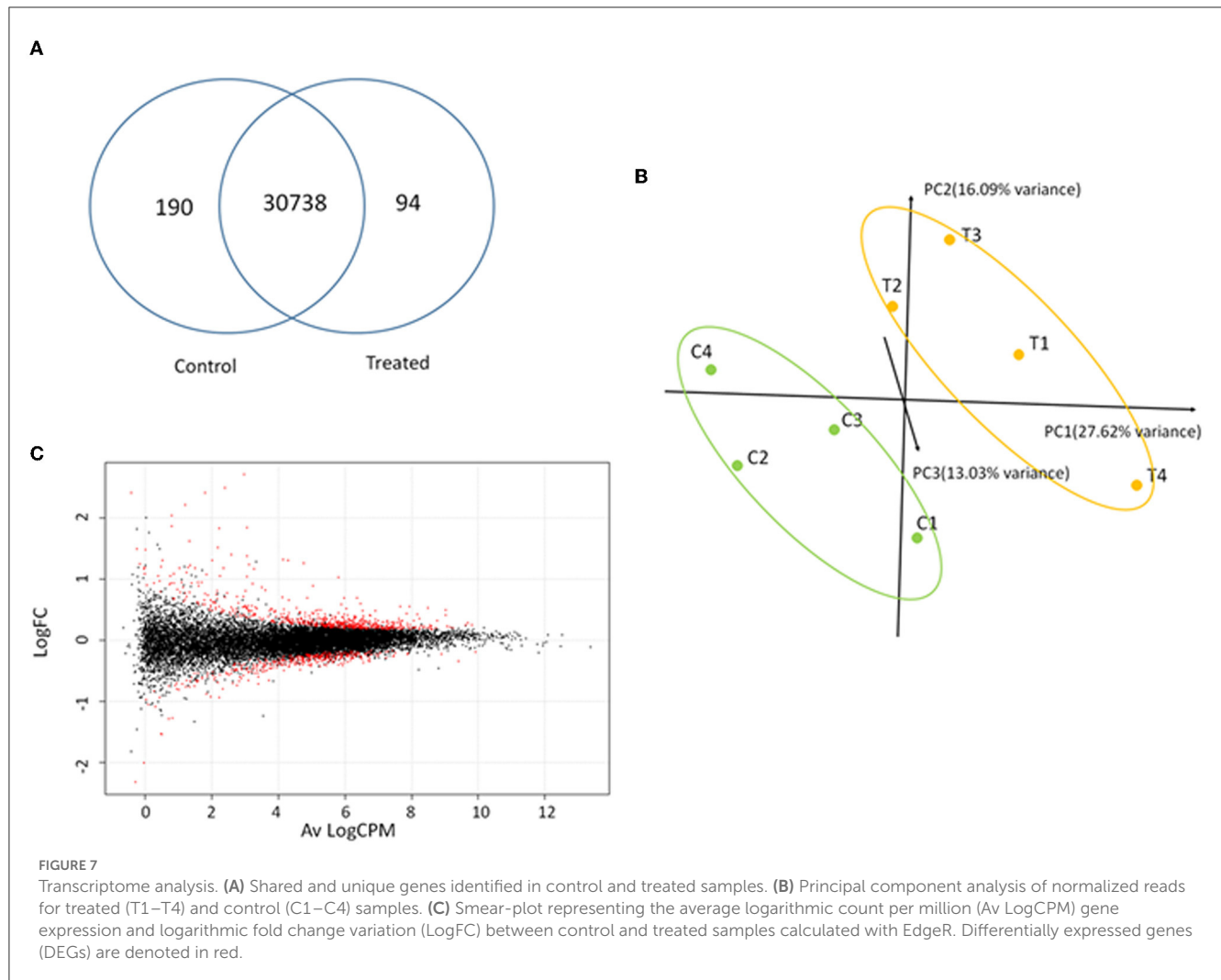


**FIGURE 6** BoHV-4 recombinant reconstitution and replication. **(A)** Representative images (phase contrast, fluorescence, and merged; 10×) of BEK cells electroperated with pBAC-BoHV-4-A, pBAC-BoHV-4-A-revORF45HA, and pBAC-BoHV-4-A-ΔORF45KanaGalK. CPE induced by reconstitution of infectious replicating viral particles (IRVPs) is recognizable only for pBAC-BoHV-4- and pBAC-BoHV-4-A-revORF45HA as revealed by green plaques. **(B)** Replication kinetics of BoHV-4-A and BAC-BoHV-4-A-revORF45. **(C)** Western immunoblotting of BoHV-4-A and BoHV-4-A-revORF45HA infected cell extracts. **(D)** Western immunoblotting of BoHV-4-A and BoHV-4-A-revORF45HA purified virus extract. All experiments were repeated three times with identical results.



tegument proteins were based on resistance to protease digestion in the absence of detergent and susceptibility to protease digestion following treatment with envelope-dissolving detergent. BoHV-4 ORF45 sequence similarity with other previously characterized *Rhadinovirus* ORF45s was not strong enough for attributing with certainty structural and functional characteristics of an authentic ORF45, mainly in the absence of experimental data. In this study, when the BoHV-4 ORF45 amino-terminal region was compared with that of KHSV ORF45, it allowed the prediction of a structure with potentially similar functions and interactive pathways to those of KHSV ORF45. Overexpression of HA-tagged or GFP-fused BoHV-4 ORF45, by transient transfection and in the absence of infection, was identified as a phosphoprotein that localizes to the host cell nucleus as was the case for KSHV, RRV, and MHV68. By construction and analysis of a BoHV-4 ORF45-null mutant and its pararevertant, using the BAC system, it was demonstrated that the ORF45 null mutant was incapable of production of virions, indicating that newly synthesized ORF45 is essential for BoHV-4 lytic replication and that such a defect could be rescued *in cis* by reintroducing ORF45. Moreover, the HA-tagged ORF45 pararevertant virus allowed to experimentally demonstrate that BoHV-4 ORF45 is associated with the virus particle, corroborating

the notion, previously partially demonstrated (Lete et al., 2012), of BoHV-4 ORF45 as part of the tegument. Tegument proteins are not just structural viral proteins that are essentially implicated in viral entry, replication, morphogenesis, and egress. They are the first viral proteins to be delivered inside the host cells immediately after virus attachment, membrane fusion, and uncoating. They can specifically modify, for increasing infection fitness, the host intracellular environment during the establishment of *de novo* infection and modify, through a specific interactome, host signaling, epigenetics, and transcriptome (Sathish et al., 2012; Atyeo and Papp, 2022). KSHV ORF45 is one of the most if not the most, investigated *Gammaherpesvirus* tegument proteins, as well as its interaction with p90 ribosomal S6 kinase (RSK) and signal-regulated kinase (ERK) complex (RSK/ERK). Since the BoHV-4 ORF45 structure was well-superimposed (RMSD 0.1 Å) on the corresponding KHSV ORF45 ortholog, the key Val and Phe (VP) interacting motif residues are also conserved in the BoHV-4 ORF45 and well fit the hydrophobic pocket located in the N-terminal of AGC-type kinase domain (NTK) of RSK, similar function for BoHV-4 ORF45 could be envisioned. ORF45 sustains activation of the p90 ribosomal S6 kinase (RSK), signal-regulated kinase (ERK), and MAP kinase pathways by binding to

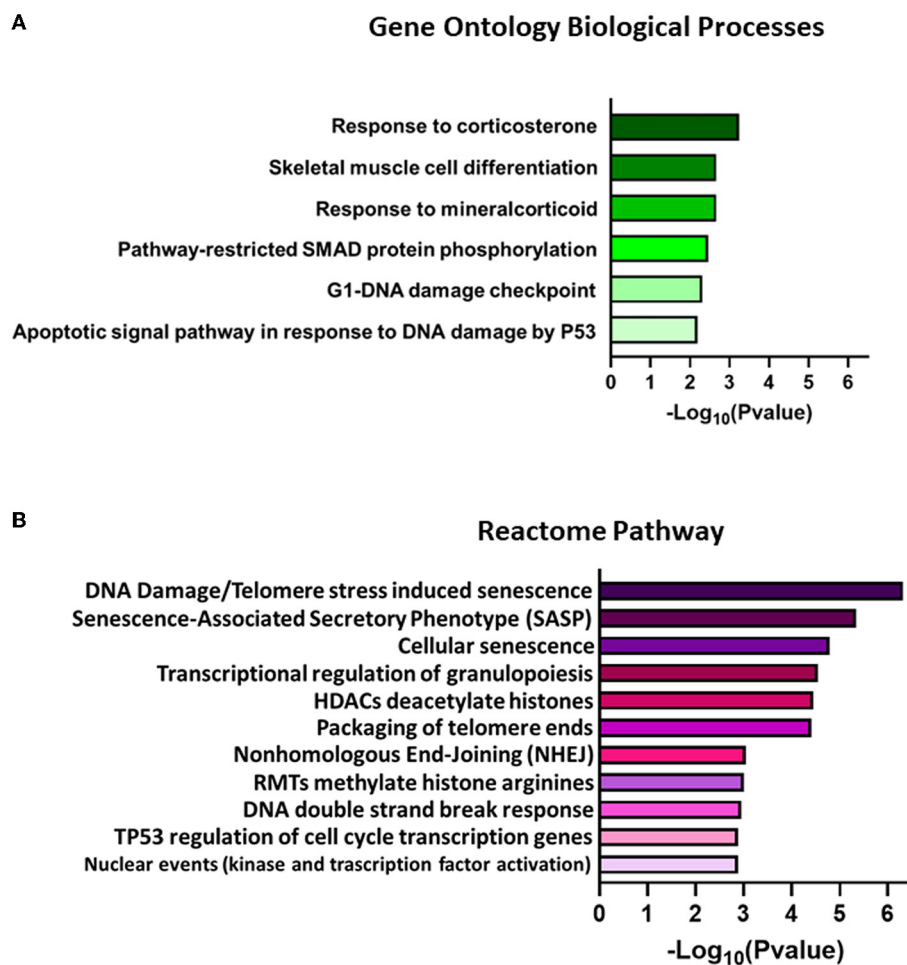


FIGURE 8

Representation of significantly enriched terms found for (A) biological processes in Gene Ontology (GO) analysis and (B) Reactome pathways for DEGs with  $\text{FDR} < 0.01$  and  $\text{LogFC} \geq 0.5$ . The elements are ordered from higher to lower  $-\text{Log}_{10}(\text{P-value})$  values. Only the best  $P$ -value scores for each identical gene group are reported in the graph bar. The complete list of associated gene groups is reported in [Supplementary Table 4](#).

the RSK/ERK complex and preventing their dephosphorylation (Kuang et al., 2009; Alexa et al., 2022) or acting as a SUMO ligase and SUMOylates RSK to promote its kinase activity (Liu et al., 2022). One of the downstream targets of the phosphorylated RSK/ERK complex is cellular transcription, which is mediated by the direct phosphorylation of transcription factors. RSKs regulate several transcription factors, including CREB, serum response factor (SRF), ER81, estrogen receptor- $\alpha$  (ER $\alpha$ ), nuclear factor- $\kappa$ B (NF- $\kappa$ B), NFATc4, NFAT3, and the transcription initiation factor TIF1A (Romeo et al., 2012). Based on this information, it was of interest to investigate the impact of BoHV-4 ORF45 on the cellular transcriptome, which was less studied or not studied at all for ORF45 belonging to other *Gammaherpesvirus*. Using stringent selection (DEGs;  $\text{FDR} < 0.01$  and  $\text{LogFC} < |0.5|$ ) for biological pathway identification, GO analysis, and Reactome pathway database interrogation, a strong transcriptome alteration was identified in cells expressing BoHV-4 ORF45. Among the most remarkable are stress response, cell differentiation, pathways restricted to SMAD protein phosphorylation, and TP53 regulation of transcription of cell cycle genes and DNA damage checkpoint

pathways in cells expressing BoHV-4 ORF45 that are consistent with cellular functional modulation in response to RSK/ERK activation. In fact, RSK binds and enhances the function of the transcriptional co-activators CREB-binding protein (CBP) and p300 (Nakajima et al., 1996; Wang et al., 2003). These proteins are large, homologous molecules that facilitate complex formation between different components of the transcriptional machinery. Among the transcription factors that associate with CBP and p300 are cAMP response element-binding protein (CREB), Fos proto-oncogene, AP-1 transcription factor subunit FOS, Jun proto-oncogene, AP-1 transcription factor subunit JUN, signal transducer and activator of transcription (STAT), myogenic differentiation protein (MyoD), E2F transcription factor (E2F), NF- $\kappa$ B, and steroid receptors, including estrogen receptor alpha (ER $\alpha$ ; Romeo et al., 2012). Among the top 200 most significant DEGs, CREB5, FOS, FOSL1, JUN, and NFKBIL1 genes showed variation in two groups of C and T samples. These transcription factors could be directly and indirectly associated with one of the pathways that are transcriptionally impacted by BoHV-4 ORF45; for instance, MyoD with cell differentiation (Noda et al.,

2009); CREB/FOS/JUN with TP53 regulates transcription of cell cycle genes (Schreiber et al., 1999; Giebler et al., 2000); NF- $\kappa$ B and CREB with pathways restricted to SMAD (Freudlsperger et al., 2013); E2F with cell cycle progression, DNA repair, replication, and G/M checkpoints (Ren et al., 2002); CREB/Er $\alpha$  with corticosteroid stress response (Jing et al., 2016). Finally, we also observed upregulation of the ETS variant transcription factors, ETV4 and ETV5, in cells expressing BoHV-4 ORF45, likely associated with RSK/ERK activation. A previous study in cancer cell lines reported that  $\alpha$ v $\beta$ 3 integrin signaling might activate the ERK pathway, resulting in ETV4 transcription, PD-L1/L2 expression, and evasion attacks from the immune system (Ma et al., 2021). Expression of endogenous retroviruses envelope protein in different human cancer cell lines was observed to induce the transcription of ETV4 and ETV5, which are downstream effectors of the MAPK ERK1/2 (Lemaitre et al., 2017). In conclusion, in the present study, for the first time, a general characterization from the structural and functional point of view of BoHV-4 ORF45 was obtained, posing the basis for further investigation on each of the characteristics pointed out here. However, in general, BoHV-4 ORF45 characteristics can be ascribed to those of KHSV ORF45.

## Data availability statement

The datasets presented in this study can be found in online repositories. The names of the repository/repositories and accession number(s) can be found at: NCBI—PRJNA938412.

## Author contributions

GD designed the experiments, wrote the manuscript, and supervised the project. LR, EC, VF, RS, DC, BL, and GD performed the experiments and analyzed the data.

## References

- Alexa, A., Sok, P., Gross, F., Albert, K., Kobori, E., Poti, A. L., et al. (2022). A non-catalytic herpesviral protein reconfigures ERK-RSK signaling by targeting kinase docking systems in the host. *Nat. Commun.* 13, 472. doi: 10.1038/s41467-022-28109-x
- Atyeo, N., and Papp, B. (2022). The ORF45 protein of Kaposi's sarcoma-associated herpesvirus and its critical role in the viral life cycle. *Viruses* 14, 92010. doi: 10.3390/v14092010
- Barahona, H. H., Trum, B. F., Melendez, L. V., Garcia, F. G., King, N. W., Daniel, M. D., et al. (1973). A new herpesvirus isolated from kinkajous (*Potos flavus*). *Lab. Anim. Sci.* 23, 830–836.
- Blom, N., Gammeltoft, S., and Brunak, S. (1999). Sequence and structure-based prediction of eukaryotic protein phosphorylation sites. *J. Mol. Biol.* 294, 1351–1362. doi: 10.1006/jmbi.1999.3310
- Blom, N., Sicheritz-Ponten, T., Gupta, R., Gammeltoft, S., and Brunak, S. (2004). Prediction of post-translational glycosylation and phosphorylation of proteins from the amino acid sequence. *Proteomics* 4, 1633–1649. doi: 10.1002/pmic.200300771
- Bublot, M., Dubuisson, J., Van Bresseem, M. F., Danyi, S., Pastoret, P. P., and Thiry, E. (1991). Antigenic and genomic identity between simian herpesvirus aotus type 2 and bovine herpesvirus type 4. *J. Gen. Virol.* 72, 715–719. doi: 10.1099/0022-1317-72-3-715
- Dewals, B., Gillet, L., Gerdes, T., Taracha, E. L., Thiry, E., and Vanderplassen, A. (2005). Antibodies against bovine herpesvirus 4 are highly prevalent in wild African buffaloes throughout eastern and southern Africa. *Vet. Microbiol.* 110, 209–220. doi: 10.1016/j.vetmic.2005.08.006
- Dewals, B., Thirion, M., Markine-Goriaynoff, N., Gillet, L., de Fays, K., Minner, F., et al. (2006). Evolution of bovine herpesvirus 4: Recombination and transmission between African buffalo and cattle. *J. Gen. Virol.* 87, 1509–1519. doi: 10.1099/vir.0.81757-0
- Dobin, A., Davis, C. A., Schlesinger, F., Drenkow, J., Zaleski, C., Jha, S., et al. (2013). STAR: Ultrafast universal RNA-seq aligner. *Bioinformatics* 29, 15–21. doi: 10.1093/bioinformatics/bts635
- Donofrio, G., Cavaggioni, A., Bondi, M., Cavarani, S., Flammini, C. F., and Mucignat-Caretta, C. (2006). Outcome of bovine herpesvirus 4 infection following direct viral injection in the lateral ventricle of the mouse brain. *Microbes Infect.* 8, 898–904. doi: 10.1016/j.micinf.2005.10.016
- Donofrio, G., Cavarani, S., Simone, T., and van Santen, V. L. (2002). Potential of bovine herpesvirus 4 as a gene delivery vector. *J. Virol. Methods* 101, 49–61. doi: 10.1016/S0166-0934(01)00419-0
- Donofrio, G., Sartori, C., Franceschi, V., Capocéfalo, A., Cavarani, S., Taddei, S., et al. (2008). Double immunization strategy with a BoHV-4-vectorialized secreted chimeric peptide BVDV-E2/BoHV-1-gD. *Vaccine* 26, 6031–6042. doi: 10.1016/j.vaccine.2008.09.023

## Funding

This research was supported by the internal fund of Parma University.

## Acknowledgments

We would like to thank Parma University for funding the project.

## Conflict of interest

The authors declare that the research was conducted in the absence of any commercial or financial relationships that could be construed as a potential conflict of interest.

## Publisher's note

All claims expressed in this article are solely those of the authors and do not necessarily represent those of their affiliated organizations, or those of the publisher, the editors and the reviewers. Any product that may be evaluated in this article, or claim that may be made by its manufacturer, is not guaranteed or endorsed by the publisher.

## Supplementary material

The Supplementary Material for this article can be found online at: <https://www.frontiersin.org/articles/10.3389/fmicb.2023.1171770/full#supplementary-material>

- Donofrio, G., Sartori, C., Ravanetti, L., Cavirani, S., Gillet, L., Vanderplasschen, A., et al. (2007). Establishment of a bovine herpesvirus 4 based vector expressing a secreted form of the bovine viral diarrhoea virus structural glycoprotein E2 for immunization purposes. *BMC Biotechnol.* 7, 68. doi: 10.1186/1472-6750-7-68
- Egyed, L., Kluge, J. P., and Bartha, A. (1997). Histological studies of bovine herpesvirus type 4 infection in non-ruminant species. *Vet. Microbiol.* 57, 283–289. doi: 10.1016/S0378-1135(97)00105-3
- Franceschi, V., Capocéfalo, A., Cavirani, S., and Donofrio, G. (2013). Bovine herpesvirus 4 glycoprotein B is indispensable for lytic replication and irreplaceable by VSVg. *BMC Vet. Res.* 9, 6. doi: 10.1186/1746-6148-9-6
- Freudspurger, C., Bian, Y., Contag Wise, S., Burnett, J., Coupar, J., Yang, X., et al. (2013). TGF-beta and NF-kappaB signal pathway cross-talk is mediated through TAK1 and SMAD7 in a subset of head and neck cancers. *Oncogene* 32, 1549–1559. doi: 10.1038/onc.2012.171
- Fu, B., Kuang, E., Li, W., Avey, D., Li, X., Turpin, Z., et al. (2015). Activation of p90 ribosomal S6 kinases by ORF45 of Kaposi's sarcoma-associated herpesvirus is critical for optimal production of infectious viruses. *J. Virol.* 89, 195–207. doi: 10.1128/JVI.01937-14
- Giebler, H. A., Lemasson, I., and Nyborg, J. K. (2000). p53 recruitment of CREB binding protein mediated through phosphorylated CREB: A novel pathway of tumor suppressor regulation. *Mol. Cell Biol.* 20, 4849–4858. doi: 10.1128/MCB.20.13.4849-4858.2000
- Jia, Q., Chernishof, V., Bortz, E., McHardy, I., Wu, T. T., Liao, H. I., et al. (2005). Murine gammaherpesvirus 68 open reading frame 45 plays an essential role during the immediate-early phase of viral replication. *J. Virol.* 79, 5129–5141. doi: 10.1128/JVI.79.8.5129-5141.2005
- Jing, Y. P., Wang, D., Han, X. L., Dong, D. J., Wang, J. X., and Zhao, X. F. (2016). The steroid hormone 20-hydroxycyclopropane enhances gene transcription through the cAMP response element-binding protein (CREB) signaling pathway. *J. Biol. Chem.* 291, 12771–12785. doi: 10.1074/jbc.M115.706028
- Kuang, E., Wu, F., and Zhu, F. (2009). Mechanism of sustained activation of ribosomal S6 kinase (RSK) and ERK by kaposi sarcoma-associated herpesvirus ORF45: Multiprotein complexes retain active phosphorylated ERK AND RSK and protect them from dephosphorylation. *J. Biol. Chem.* 284, 13958–13968. doi: 10.1074/jbc.M900025200
- Lemaitre, C., Tsang, J., Bireau, C., Heidmann, T., and Dewannieux, M. (2017). A human endogenous retrovirus-derived gene that can contribute to oncogenesis by activating the ERK pathway and inducing migration and invasion. *PLoS Pathog.* 13, e1006451. doi: 10.1371/journal.ppat.1006451
- Lete, C., Palmeira, L., Leroy, B., Mast, J., Machiels, B., Wattiez, R., et al. (2012). Proteomic characterization of bovine herpesvirus 4 extracellular virions. *J. Virol.* 86, 11567–11580. doi: 10.1128/JVI.00456-12
- Li, H., Gailbreath, K., Flach, E. J., Taus, N. S., Cooley, J., Keller, J., et al. (2005). A novel subgroup of rhadinoviruses in ruminants. *J. Gen. Virol.* 86, 3021–3026. doi: 10.1099/vir.0.81238-0
- Li, X., and Zhu, F. (2009). Identification of the nuclear export and adjacent nuclear localization signals for ORF45 of Kaposi's sarcoma-associated herpesvirus. *J. Virol.* 83, 2531–2539. doi: 10.1128/JVI.02209-08
- Liu, Z., Wang, X., Liu, C., Deng, H., Li, W., Wang, X., et al. (2022). The SUMO E3 ligase activity of ORF45 determines KSHV lytic replication. *PLoS Pathog.* 18, e1010504. doi: 10.1371/journal.ppat.1010504
- Ma, P., Jin, X., Fan, Z., Wang, Z., Yue, S., Wu, C., et al. (2021). Super-enhancer receives signals from the extracellular matrix to induce PD-L1-mediated immune evasion via integrin/BRAF/TAK1/ERK/ETV4 signaling. *Cancer Biol. Med.* 19, 669–684. doi: 10.20892/j.issn.2095-3941.2021.0137
- McGeoch, D. J., Dolan, A., and Ralph, A. C. (2000). Toward a comprehensive phylogeny for mammalian and avian herpesviruses. *J. Virol.* 74, 10401–10406. doi: 10.1128/JVI.74.22.10401-10406.2000
- Moreno-Lopez, J., Goltz, M., Rehbinder, C., Valsala, K. V., and Ludwig, H. (1989). A bovine herpesvirus (BHV-4) as passenger virus in ethmoidal tumours in Indian cattle. *Zentralbl. Veterinarmed. B* 36, 481–486. doi: 10.1111/j.1439-0450.1989.tb00633.x
- Nakai, K. (2000). Protein sorting signals and prediction of subcellular localization. *Adv. Protein Chem.* 54, 277–344. doi: 10.1016/S0065-3233(00)54009-1
- Nakajima, T., Fukamizu, A., Takahashi, J., Gage, F. H., Fisher, T., Blenis, J., et al. (1996). The signal-dependent coactivator CBP is a nuclear target for pp90RSK. *Cell* 86, 465–474. doi: 10.1016/S0092-8674(00)80119-1
- Noda, T., Fujino, T., Mie, M., and Kobatake, E. (2009). Transduction of MyoD protein into myoblasts induces myogenic differentiation without addition of protein transduction domain. *Biochem. Biophys. Res. Commun.* 382, 473–477. doi: 10.1016/j.bbrc.2009.03.060
- Palmeira, L., Machiels, B., Lete, C., Vanderplasschen, A., and Gillet, L. (2011). Sequencing of bovine herpesvirus 4 v.test strain reveals important genome features. *Viral J.* 8, 406. doi: 10.1186/1743-422X-8-406
- Pettersen, E. F., Goddard, T. D., Huang, C. C., Meng, E. C., Couch, G. S., Croll, T. I., et al. (2021). UCSF ChimeraX: Structure visualization for researchers, educators, and developers. *Protein Sci.* 30, 70–82. doi: 10.1002/pro.3943
- Purdy, M. A., Drexler, J. F., Meng, X. J., Norder, H., Okamoto, H., Van der Poel, W. H. M., et al. (2022). ICTV virus taxonomy profile: hepeviridae 2022. *J. Gen. Virol.* 103, 1778. doi: 10.1099/jgv.0.001778
- Ren, B., Cam, H., Takahashi, Y., Volkert, T., Terragni, J., Young, R. A., et al. (2002). E2F integrates cell cycle progression with DNA repair, replication, and G(2)/M checkpoints. *Genes Dev.* 16, 245–256. doi: 10.1101/gad.949802
- Roizmann, B., Desrosiers, R. C., Fleckenstein, B., Lopez, C., Minson, A. C., and Studdert, M. J. (1992). The family Herpesviridae: an update. The Herpesvirus Study Group of the International Committee on taxonomy of viruses. *Arch. Virol.* 123, 425–449. doi: 10.1007/BF01317276
- Romeo, Y., Zhang, X., and Roux, P. P. (2012). Regulation and function of the RSK family of protein kinases. *Biochem. J.* 441, 553–569. doi: 10.1042/BJ20110289
- Sathish, N., Wang, X., and Yuan, Y. (2012). Tegument proteins of Kaposi's sarcoma-associated herpesvirus and related gamma-herpesviruses. *Front. Microbiol.* 3, 98. doi: 10.3389/fmicb.2012.00098
- Schreiber, M., Kolbus, A., Piu, F., Szabowski, A., Mohle-Steinlein, U., Tian, J., et al. (1999). Control of cell cycle progression by c-Jun is p53 dependent. *Genes Dev.* 13, 607–619. doi: 10.1101/gad.13.5.607
- Sturm, A., Quackenbush, J., and Trajanoski, Z. (2002). Genesis: cluster analysis of microarray data. *Bioinformatics* 18, 207–208. doi: 10.1093/bioinformatics/18.1.207
- Wang, Z., Zhang, B., Wang, M., and Carr, B. I. (2003). Persistent ERK phosphorylation negatively regulates cAMP response element-binding protein (CREB) activity via recruitment of CREB-binding protein to pp90RSK. *J. Biol. Chem.* 278, 11138–11144. doi: 10.1074/jbc.M209108200
- Warming, S., Costantino, N., Court, D. L., Jenkins, N. A., and Copeland, N. G. (2005). Simple and highly efficient BAC recombineering using galK selection. *Nucleic Acids Res.* 33, e36. doi: 10.1093/nar/gni035
- Waterhouse, A., Bertoni, M., Bienert, S., Studer, G., Tauriello, G., Gumienny, R., et al. (2018). SWISS-MODEL: homology modelling of protein structures and complexes. *Nucleic Acids Res.* 46, W296–W303. doi: 10.1093/nar/gky427
- Webb, B., and Sali, A. (2016). Comparative protein structure modeling using MODELLER. *Curr. Protoc. Bioinform.* 54, 1–37. doi: 10.1002/cpbi.3
- Zhu, F. X., and Yuan, Y. (2003). The ORF45 protein of Kaposi's sarcoma-associated herpesvirus is associated with purified virions. *J. Virol.* 77, 4221–4230. doi: 10.1128/JVI.77.7.4221-4230.2003
- Zimmermann, W., Broll, H., Ehlers, B., Buhk, H. J., Rosenthal, A., and Goltz, M. (2001). Genome sequence of bovine herpesvirus 4, a bovine Rhadinovirus, and identification of an origin of DNA replication. *J. Virol.* 75, 1186–1194. doi: 10.1128/JVI.75.3.1186-1194.2001